Published in final edited form as:

Cancer Res. 2017 February 01; 77(3): 613–622. doi:10.1158/0008-5472.CAN-16-1298.

Differential regulation of the melanoma proteome by eIF4A1 and eIF4E

Cailin E. Joyce[1,2,3], **Adrienne G. Yanez**[1,2,3], **Akihiro Mori**[4,5,6], **Akinori Yoda**[1,2,3], **Johanna S. Carroll**[1,2,3], and **Carl D. Novina**[1,2,3,†]

[1]Department of Cancer Immunology and Virology, Dana-Farber Cancer Institute, Boston, MA 02115

[2]Department of Microbiology and Immunobiology, Harvard Medical School, Boston, MA 02115

[3]Broad Institute of Harvard and MIT, Cambridge, MA 02141

[4]Program in Systems Biology and Program in Molecular Medicine, University of Massachusetts, Worcester, MA 01605

[5]Onami team, The Systems Biology Institute, Tokyo, Japan

[6]Laboratory for Developmental Dynamics, RIKEN Quantitative Biology Center, Hyogo, Japan

Abstract

Small molecules and antisense oligonucleotides that inhibit the translation initiation factors eIF4A1 and eIF4E have been explored as broad-based therapeutic agents for cancer treatment, based on the frequent upregulation of these two subunits of the eIF4F cap-binding complex in many cancer cells. Here we provide support for these therapeutic approaches with mechanistic studies of eIF4F-driven tumor progression in a preclinical model of melanoma. Silencing eIF4A1 or eIF4E decreases melanoma proliferation and invasion. There were common effects on the level of cell cycle proteins which could explain the antiproliferative effects in vitro. Using clinical specimens, we correlate the common cell cycle targets of eIF4A1 and eIF4E with patient survival. Finally, comparative proteomic and transcriptomic analyses reveal extensive mechanistic divergence in response to eIF4A1 or eIF4E silencing. Current models indicate that eIF4A1 and eIF4E function together through the 5′UTR to increase translation of oncogenes. In contrast, our data demonstrate that the common effects of eIF4A1 and eIF4E on translation are mediated by the coding region and 3′UTR. Moreover, their divergent effects occur through the 5′UTR. Overall, our work shows that it will be important to evaluate subunit-specific inhibitors of eIF4F in different disease contexts to fully understand their anticancer actions.

Keywords

Melanoma; proteomics; translation; cell cycle; patient survival

[†]corresponding author: Carl D. Novina, Dana-Farber Cancer Institute, Dana 1420B, 450 Brookline Avenue, Boston, MA 02215, carl_novina@dfci.harvard.edu, Tel: 617-582-7961, Fax: 617-582-7962.

CONFLICT OF INTEREST STATEMENT: The authors declare no conflict of interest.

INTRODUCTION

Steady state translation initiation is primarily regulated through the cytoplasmic mRNA cap binding complex, eukaryotic initiation factor 4F (eIF4F), comprised of the cap binding protein eIF4E, the RNA helicase eIF4A and the scaffolding protein eIF4G (reviewed in (1)). Increased protein levels of eIF4E (2), phospho-eIF4E (3), eIF4A1 (4) and eIF4G (5) are associated with poor clinical outcomes in multiple cancer contexts and are linked to aggressive phenotypes in cellular and preclinical models (6–8). In melanoma, many of the known oncogenic signaling pathways converge on eIF4F (9). Targeted therapies that deactivate these pathways are initially effective, but nearly universal acquired resistance leads to high mortality rates (10). Thus, second-line inhibition of eIF4F could significantly extend the period of response to targeted therapies for melanoma patients.

Classic models dictate that eIF4E is the rate-limiting factor for translation initiation in most normal tissues (11). Under physiological conditions, mRNAs are thought to compete for limiting amounts of eIF4E. In this model, mRNAs with longer and more structured 5′UTRs are weakly translated. In cancer cells, increased availability of eIF4E leads to selective translation of highly-sensitive oncogenes, such as MYC (12) and VEGF (13). More recently, this model was extended to incorporate 5′UTR sequence elements that confer eIF4E sensitivity such as the terminal oligonucleotide tract (5′TOP), pyrimidine-rich translational element (PRTE) and cytosine-enriched regulator of translation (CERT) (14–16). However, 5′UTR features do not explain the full spectrum of eIF4E targets (17), including the class of mRNAs for which eIF4E negatively regulates translation. Improved models are necessary to predict outcomes of therapeutic inhibition of eIF4F in cancer.

Targets of eIF4A and eIF4E have been identified using polysomal RNA association or ribosome profiling to estimate translation efficiency (16,18–21). Some mRNAs have different requirements for individual eIF4F subunits (19,22), but global effects of eIF4A1 and eIF4E depletion have not been assessed in parallel in the same cancer model. Here, we characterize the phenotypic and global proteomic effects of eIF4A1 and eIF4E inhibition in melanoma. We show that eIF4A1 and eIF4E promote melanoma proliferation through shared, network-level regulation of the cell cycle, and moreover, that eIF4F-dependent cell cycle proteins are significant combinatorial predictors of patient survival. Finally, we demonstrate that intrinsic features of mRNA coding sequence (CDS) and 3′UTR, but not 5′UTR, predict shared targets of eIF4A1 and eIF4E. These data demonstrate that eIF4A1 and eIF4E have distinct molecular consequences in the same cancer model, which implies that targeting eIF4F with different subunit-specific inhibitors will influence on-target and off-target therapeutic outcomes.

MATERIALS AND METHODS

Additional methods are provided in supplementary file S1.

Cell culture

WM858, WM46 and A375 were cultured in high glucose DMEM (Cellgro) supplemented with 10% fetal bovine serum (Life Technologies). WM46 was transduced with lentivirus

containing empty SparQ IRES RFP vector (QM531A-2, System Biosciences), or vector containing eIF4A1 (4096621, Open Biosystems) or eIF4E cDNA (5295521, Open Biosystems). RFP positive cells in the middle quantiles were selected by flow cytometry. The A375 melanoma cell line was a gift from Dr. David Fisher, and WM46 and WM858 were a gift from Dr. Levi Garraway, all obtained prior to 2012. All cell lines were authenticated via short tandem repeat profiling at the American Tissue Culture Repository on May 19, 2016.

Transient knockdown

A375 and WM858 cells were transfected with Allstars Negative Control siRNA (Qiagen) or gene-specific siRNA at 7.5 nM using RNAiMAX (Life Technologies). Gene-specific siRNA sequences were 5′-GCATGGAGATATCTCCATGCAT and 5′-GCATGGAGATATGGACCAATT for eIF4A1 (custom design, Qiagen) and 5′-AAGAGCGGCTCCACCACTAAA and 5′-CAAAGCTTTGCTACAAATTTA for eIF4E (Hs_EIF4E_1 and Hs_EIF4E_8, Qiagen). siRNA-like off-target effects were assessed by siRNA-check (http://projects.insilico.us/SpliceCenter/siRNACheck). miRNA-like off-target effects were assessed by scanning 3′UTRs for perfect matches to the 8-mer seed region of each oligonucleotide (underlined above).

Proliferation assays

2500 cells per well were seeded into 96-well plates and, where appropriate, transfected with siRNA. After 24 hours (h), cell culture medium was replaced with 10μl Wst-1 (Pierce) in 100μl complete medium. Cells were incubated in growth conditions for 30 minutes, and absorbance was measured at 450 nm on a Victor 3V plate reader (Perkin Elmer). Additional readings were taken at 48, 72 and 96h. Blank readings were subtracted from test readings and net absorbance values were plotted relative to the 24h time point. Significance was calculated by two-way ANOVA with Dunnett's multiple correction test (GraphPad Prism v7.0).

Invasion assays

4.0×10^4 (knockdown) or 2.0×10^4 (overexpression) cells were washed and resuspended in serum free medium. Cells were seeded in rehydrated control or Matrigel invasion chambers (BD Biocoat), chambers were placed in wells of a 24-well plate containing 750μl DMEM supplemented with 30% FBS, and plates were incubated under growth conditions for 20h. Non-migratory cells were removed by scrubbing twice with a cotton swab. Filters were washed in cold PBS, fixed in cold 100% methanol and mounted with Vectashield Hard Set Mounting Medium with DAPI (Vector Labs). Eight visual fields were photographed for cell counting. Invasion assays were performed 48h post-transfection and 4 hours post-treatment with 1uM rotenone, when applicable. Significance was calculated by one-way ANOVA with Dunnett's multiple correction test (GraphPad Prism v7.0).

Quantitative mass spectrometry

Knockdowns were performed in triplicate in 10cm dishes and cells were collected 72h post-transfection. Samples were processed and analyzed for MS3 mass spectrometry as

previously described (23). Briefly, cells were lysed, proteins were digested using LysC and trypsin, and peptides were labeled with Tandem Mass Tag 10-plex reagents and fractionated. Data were collected on an Orbitrap Fusion mass spectrometer operating in MS3 mode using synchronous precursor selection for MS2 to MS3 fragmentation, and forward and reverse sequences were searched against a Uniprot human database (February 2014) using the SEQUEST algorithm. Additional processing steps included protein assembly and quantification from peptides, and calculation of Benjamini-Hochberg false discovery rates (FDR). Protein levels were normalized to the percent signal in each sample relative to the total signal across all multiplexed samples. Differentially expressed proteins had a fold change ≥|1.25| in all three biological replicates and FDR <0.1 in primary and secondary siRNA treatments.

Pathway and network analysis

Gene set enrichment analysis was performed using GSEA (http://software.broadinstitute.org/gsea/index.jspGene). Differentially expressed proteins for each treatment were ranked based on their average fold-change across triplicates and analyzed against Reactome pathways (http://www.reactome.org/pathways) using the GSEA Preranked tool. We applied a classic enrichment statistic, filtered gene sets with >500 or <15 hits, and applied an FDR threshold ≤0.1. To visualize enrichment of common pathways, we ranked all genes based on their average fold-change across all knockdown treatments and performed GSEA Preranked as above. The normalized enrichment score calculates the degree to which a gene set is overrepresented at the extremes of a ranked list, accounting for size of the gene set. To predict functional outcomes of differentially expressed genes, we used the Diseases and Functions tool in Ingenuity Pathway Analysis (IPA; Qiagen). Differentially expressed cell cycle proteins were assigned to cell cycle phases based on their membership in Reactome daughter categories under the cell cycle parent category.

Cell cycle analysis

Knockdowns were performed in 6 well dishes. Cells were collected 72 hours post-transfection, washed once in PBS, fixed in 70% ethanol for 30 min at 4°C pelleted pelleted at 850xg for 10 min, and washed again in PBS. Pellets were resuspended in 50ul 100ug/ml RNase A and incubated at room temperature for 15 min. 200ul 50ug/ml propidium iodide was added and the suspension was incubated in the dark at room temperature for 20 min. Cells were passed through a cell strainer filter and analyzed on a BD LSR II FACS machine. Proportions of G1, S and G2 cells were assessed in FlowJo v10. Significance was calculated by two-way ANOVA with Dunnett’s multiple correction test (GraphPad Prism v7.0).

Apoptosis assays

Knockdowns were performed in 6 well dishes. Cells were collected 48 or 72 hours post-transfection, stained with the Pacific Blue Annexin V Apoptosis Detection Kit (Biolegend) and analyzed on a BD LSR II FACS machine. Proportions of ANXAV- and propidium iodide-positive cells were assessed in FlowJo v10. Significance was calculated by two-way ANOVA with Dunnett’s multiple correction test (GraphPad Prism v7.0).

Patient survival

Clinical and protein expression data (level 3; normalized expression) were obtained for skin cutaneous melanoma patients in TCGA. All protein data were generated by the Reverse Phase Protein Array Core Facility at MD Anderson Cancer Center (Houston, TX), providing adequate internal control among samples. Significance of Kaplan-Meier survival curves was calculated using the Gehan-Breslow-Wilcoxon test, which does not assume equivalent proportional hazards over time (GraphPad Prism software v7.0).

RNA sequencing (RNA-seq)

Knockdowns were performed in duplicate in 10cm dishes. RNA was extracted 72 hours post-transfection using Trizol reagent. cDNA libraries were prepared from 1ug total RNA using the Illumina TruSeq RNA sample preparation kit, v2. Raw counts were obtained using the Python package ‘HTSeq-count’, and normalized using the R package ‘deseq’. Differentially expressed mRNAs had a fold change ≥|1.25| and FDR≤0.1.

Effect size calculation

Cliff’s D was calculated using the cliff.delta function in the R package ‘effsize’. This test nonparametrically measures how often the values in one distribution are larger than those in another distribution. Significance was calculated by the Mann-Whitney-U test using the wilcox.test function in R.

miRNA reporter assays

Knockdowns were performed in triplicate in 96 well plates. 24h post-knockdown, cells were re-transfected with 100ng psiCheck2–6X-CXCR4 and 15nM si-Scr or artificial CXCR4 siRNA (5′-GUUUUCACUCCAGCUAACACA-3) using Lipofectamine 2000 (Life Technologies). Dual luciferase assays (Promega) were performed and analyzed on a Victor 3V plate reader (Perkin Elmer) 48h after reporter transfection. miRNA-targeted *Renilla* luciferase (R-luc) was normalized to untargeted firefly luciferase (F-luc) in each well. Fold repression was calculated as the R-luc:F-luc ratio in the absence of CXCR4 divided by the R-luc:F-luc ratio in the presence of CXCR4.

RESULTS

eIF4A1 and eIF4E positively regulate melanoma proliferation and invasion

We assessed the phenotypic effects of altered eIF4F expression in melanoma short-term cultures (MSTC), which are expanded directly from patient biopsies and provide an accurate representation of melanoma *in vivo* (24). The highly proliferative and invasive WM858 culture has an average doubling time of 34 hours and invasion rate of 19.5% (Fig. 1A, si-Scr). The weakly proliferative and invasive WM46 culture has an average doubling time of 62 hours and invasion rate of 6% (Fig. 1B, oe-Empty). Knockdown of eIF4A1 or eIF4E in WM858 decreased proliferation and invasion (Fig. 1A, S1A) while overexpression in WM46 increased invasion and modestly (p=0.127) increased proliferation (Fig. 1B, S1B). These data show that eIF4E and eIF4A1 positively regulate melanoma proliferation and invasion, two critical processes underlying disease progression.

eIF4A1 and eIF4E have disparate effects on the melanoma proteome

MSTCs accurately reflect melanoma biology, but they are not ideal for integrative molecular profiling because of their slow growth rates, limited proliferative capacity and variable transfectability. A375 is an immortalized, transfectable melanoma cell line that is even more invasive and proliferative than WM858 *in vitro*. We confirmed that knockdown of either eIF4A1 or eIF4E using primary and secondary siRNAs (Fig. S1C,D) reduced proliferation and invasion of A375 cells (Fig. 1C). Thus, A375 is a suitable model system in which to examine responses to eIF4F inhibition.

All previous global studies on the effects of eIF4A1 and eIF4E have relied on polysome or ribosome profiling, but technical biases have contributed to discordant results (22). Moreover, these methods do not directly assess protein levels which are more closely related to cellular phenotypes than mRNA levels or ribosome occupancy. To define the eIF4F-dependent melanoma proteome, we performed triple-stage mass spectrometry (MS3) on A375 cells depleted of eIF4A1 or eIF4E for 72 hours. We identified 1286 and 756 differentially expressed proteins in eIF4A1- or eIF4E-depleted melanomas, respectively (Fig. 2A, Table S1). eIF4A1 and eIF4E protein levels were 3.6-fold (+/−0.23, FDR=4.65×10^{-4}) and 3.3-fold (+/−0.16, FDR=1.82×10^{-3}) reduced in their respective treatments, and neither was affected by depletion of the other.

Among all proteins that were affected by eIF4F depletion (either eIF4A1 or eIF4E), only 19% (320/1706) were commonly affected by depletion of both factors (Fig. 2B). This was surprising given the shared phenotypic outcomes in eIF4A1- or eIF4E-depleted melanomas and their known physical interaction as members of the eIF4F cap-binding complex. To independently validate this result, we performed western blotting of several differentially expressed proteins (Fig. S2). As additional confirmation, we computationally predicted siRNA-like or miRNA-like off-target effects of each siRNA. There were no alternative binding sites in the human transcriptome that would lead to siRNA-like off target effects, even when allowing up to 2 mismatches. However, there were 38 decreased proteins whose mRNAs contained 8-mer miRNA seed matches to the siRNAs in their 3′UTRs. Since the siRNAs could act like miRNAs to repress translation of these proteins, we removed these genes from subsequent analyses. Overall, the vast majority of factor-specific effects were likely due to on-target depletion of eIF4A1 and eIF4E.

eIF4A1 and eIF4E promote melanoma proliferation via shared regulation of the cell cycle protein network

Despite the prevalence of factor-specific changes, we hypothesized that eIF4A1 and eIF4E depletion elicit common phenotypes via commonly dysregulated proteins. Consistent with this hypothesis, the 320 common protein changes predicted decreased proliferation ($p=1.32\times10^{-3}$, activation z-score=−2.557) and tumor progression ($p=3.82\times10^{-4}$, activation z-score=−0.728). To investigate this hypothesis further, we performed Gene Set Enrichment Analysis among differentially expressed proteins (Fig. 2C, Table S2). Three Reactome pathways were commonly enriched following depletion of either factor: Cell Cycle and related DNA Replication were decreased while the Tricarboxylic Acid Cycle and Respiratory Electron Transport Chain (TCA/ETC) was increased (Fig. 2C,D).

Core regulators of all cell cycle phases contributed to the Cell Cycle pathway enrichment (Fig. 3A), suggesting a general dampening of the pathway rather than checkpoint-specific arrest. Consistent with this, the relative proportion of cells in G0/G1, S or G2/M phase was not affected by eIF4A1 or eIF4E depletion (Fig. 3B). Reduced cell number in the absence of cell cycle phase skewing could also be due to apoptosis, but we found no evidence for increased apoptosis at 48 or 72 hours post-knockdown (Fig. S3, 3C), nor did we detect an enrichment of apoptosis pathways (Fig. 2C). Thus, we conclude that eIF4A1 and eIF4E are required to maintain the overall rate of entry and progression through the cell cycle in melanoma.

We examined the importance of eIF4F-dependent cell cycle regulation to patient outcomes in 328 cutaneous melanoma patients in The Cancer Genome Atlas (TCGA) for which reverse phase protein array data was available. We first confirmed that low expression of eIF4E (eIF4A1 was not queried on the array) conferred a survival advantage in this dataset ($p=0.0149$, Fig 3E), as has been reported elsewhere (25,26). We next identified three core cell cycle proteins queried on the array that were commonly regulated by eIF4A1 and eIF4E: CCND1, CDK1 and CCNB1 (Fig 3D). Low expression of each factor alone confers a small survival advantage that is not statistically significant (Fig. S4), but low expression of all three factors together conferred a strong advantage ($p=0.0030$, Fig. 3E). These data suggest that network-level upregulation of cell cycle proteins by eIF4A1 and eIF4E reduces melanoma patient survival.

eIF4A1 and eIF4E promote melanoma invasion via distinct mechanisms

A common mechanism underlying eIF4A1- and eIF4E-dependent invasion was less clear from the functional enrichment data. However, increased glycolysis is associated with melanoma invasion (27), which led us to hypothesize that increased expression of the alternative metabolic pathway, TCA/ETC, in eIF4A1- and eIF4E- depleted melanomas (Fig. 2D) results in a metabolic switch that reduces invasion. If true, inhibiting the ETC in the context of eIF4A1 or eIF4E depletion should restore high levels of invasion in A375. We treated cells with the ETC complex I inhibitor, rotenone, in combination with si-Scr, si-eIF4A1 or si-eIF4E. Contrary to our hypothesis, rotenone decreased invasion in the si-Scr treatment and had no effect on invasion in eIF4A1- or eIF4E-depleted cells (Fig. S5). Thus, eIF4A1 and eIF4E do not promote melanoma invasion through increased use of the TCA/ETC metabolic pathway. In fact, this pathway appears to promote invasion through an eIF4F-independent mechanism.

Because the eIF4E- and eIF4A-dependent proteomes did not reveal any common pathways of melanoma invasion, we examined whether eIF4A1 and eIF4E might reduce invasion through different mechanisms. Separate analyses of the proteomes predicted reduced invasion of tumor cell lines ($p=2.84\times10^{-12}$ and 7.42×10^{-4}, $z=-2.39$ and -1.308, for eIF4A1 and eIF4E, respectively), but the specific proteins contributing to each factor's enrichment differed. Notable examples included decreased expression of alpha and beta integrins in eIF4A1-depleted melanomas and decreased expression of epidermal growth factor receptor in eIF4E-depleted melanomas (28,29). Thus, it is likely that eIF4A1 and eIF4E commonly regulate the invasion phenotype by different molecular mechanisms.

Direct and indirect regulation by eIF4A1 and eIF4E shape the melanoma proteome

Proteomics links eIF4A1- and eIF4E-dependent phenotypes to changes in protein output, but it does not discern whether the regulatory mechanism is direct (translational) or indirect (transcriptional or post-transcriptional). Previous studies used translational profiling at very early time points to identify direct targets and mitigate effects on transcription and mRNA stability (18–21). We devised an alternate strategy that enriches for direct targets at later time points by calculating discordance between mRNA and protein fold-changes.

92% of proteins detected by MS3 were also detected at the mRNA level by RNA-seq (Fig. 4A). Among the overlapping set, 2602 mRNAs were differentially expressed using the |1.25|-fold threshold applied to the MS3 dataset (Table S3, Fig. S6A). We note that this threshold is more permissive for the RNA-seq dataset because the dynamic range of fold-changes was 2.6-times greater than that of MS3. Despite the large number of differentially expressed mRNAs, the Cell Cycle and TCA/ETC pathway enrichments were diminished at the mRNA level (Fig. S6B, Table S2). Thus, mRNA expression changes are less indicative of altered cellular processes than protein expression changes in the context of eIF4A1 and eIF4E depletion.

We next used mRNA fold-changes to infer direct and indirect protein targets of eIF4A1 and eIF4E among differentially expressed proteins. Proteins were classified as direct targets if there was no change or an opposing change in the cognate mRNA level. This method identified known direct targets (Table S4), along with many novel direct targets of both factors. In total, 76.8% (911/1186) of eIF4A1-responsive proteins and 67.5% (468/693) of eIF4E-responsive proteins were direct targets (Fig. 4B). Surprisingly, nearly half of all direct targets were negatively regulated by eIF4A1 or eIF4E (Fig. 4B, red points), suggesting a prominent role for eIF4A1 and eIF4E in translational repression which has been observed previously, but is poorly understood (16,18–21).

To investigate the relative contributions of direct and indirect regulation on the cellular processes regulated by eIF4F, we focused on commonly enriched cell cycle and TCA/ETC pathways, which are subject to opposing regulation; the cell cycle pathway was positively regulated by eIF4E and eIF4A whereas the TCA/ETC pathway was negatively regulated by eIF4E and eIF4A; (Fig. 2D). Among 56 positively-regulated cell cycle pathway members, 77% and 62% of proteins were direct targets of eIF4A1 and eIF4E, respectively (Fig. 4C). Among 23 negatively-regulated TCA/ETC pathway members, 85% and 60% of proteins were direct targets of eIF4A1 and eIF4E, respectively (Fig. 4C). Thus, eIF4A1 and eIF4E directly regulate the cell cycle by promoting translation of one set of mRNAs and directly regulate the TCA/ETC pathway by inhibiting translation of a different set of mRNAs.

5′UTR features predict selective effects of eIF4A1 and eIF4E on translation

To define mRNA-based determinants of positive and negative translational regulation by eIF4A1 and eIF4E, we calculated the effect size for intrinsic mRNA features (Fig. 5A). All significant features for direct targets had diminished or even opposing effects among indirect targets (Fig. S7), highlighting their relevance to direct translational regulation. Surprisingly, all significant features in the 5′UTR were specific to either eIF4A1 or eIF4E. eIF4A1

promotes translation of mRNAs with long, GC-rich, structured 5′UTRs which is consistent with its biochemical activity as an RNA helicase. In contrast, eIF4E promotes translation of mRNAs with shorter, less structured 5′UTRs that are depleted of upstream start codons and upstream open reading frames.

The negative correlation between 5′UTR structure and eIF4E levels contradicts earlier models (1). We examined whether the presence of eIF4E-responsive 5′UTR sequence elements could explain this discrepancy. TOP and PRTE elements (14,15) were present in less than 10% of eIF4E-dependent 5′UTRs, suggesting that they do not broadly contribute to eIF4E-dependent regulation in melanoma. The CERT element was previously identified by polysome profiling in a mouse model of eIF4E-driven oncogenic transformation (16). In our dataset, the CERT element was present in 47.9% of eIF4E-responsive 5′UTRs. Notably, the CERT element was not more prevalent among positively versus negatively regulated 5′UTRs (Fig. S8A). However, the CERT element was present at a higher density in the 5′UTRs and 3′UTRs of positively-regulated mRNAs containing the motif compared to negatively-regulated mRNAs containing the motif ($p=1.87\times10^{-2}$ and 5.11×10^{-3}, respectively; Fig. S8B). Our data independently corroborate a role for the 5′UTR CERT element in eIF4E-dependent regulation and further suggest that CERT elements may play a similar role in the 3′UTR.

Another reason that our eIF4E-responsive 5′UTRs deviate from earlier models may be that compensatory mRNA changes mask protein-level changes in the context of long-term eIF4E depletion. For example, eIF4E is known to promote translation of many ribosomal subunit proteins via 5′ UTR TOP motifs (14,15), but ribosomal subunit proteins were not downregulated in eIF4E-depleted melanoma. To investigate whether eIF4A1 or eIF4E knockdown leads to compensatory increases in mRNA levels that could mask reduction in protein levels, we examined our mRNA expression data and found dramatic upregulation of ribosomal subunits at the mRNA level (Fig. S9). This finding suggests that an increased number of transcripts compensates for the translational defect on ribosomal subunit mRNAs. Despite potential confounding factors, it appears that 5′UTR composition is the primary differentiator between eIF4A1-regulated and eIF4E-regulated transcripts.

CDS and 3′UTR features predict common translational targets of eIF4A1 and eIF4E

CDS and 3′UTR features defined common regulation by both factors. Rare codon frequency, 3′UTR length, miRNA binding site density and exon junction density were the only significant features among the shared direct targets of eIF4A1 and eIF4E (Fig. 5A). The increased density of miRNA binding sites among negatively regulated transcripts was intriguing since previous studies have implicated both eIF4E (30) and eIF4A (31) in miRNA-mediated repression. To validate this observation in a controlled setting, we tested miRNA function in A375 cells depleted of eIF4A1 or eIF4E using a dual luciferase reporter assay. Depletion of either factor reduced miRNA-mediated repression (Fig. 5C). In concert with our genome-wide analysis of shared eIF4A1 and eIF4E targets, these data establish that eIF4F negatively regulates translation via enforcement of miRNA-mediated repression in melanoma.

Taken together, our data implicate features in the CDS and 3′UTR of target mRNAs as determinants of direct targets that are common to eIF4A1 and eIF4E, whereas distinct 5′UTR features primarily determine eIF4A1- and eIF4E-specific targets. It is likely that the lack of predictive 5′UTR features among common targets reflects neutralization of the opposing 5′UTR features that determine factor-specific responses. These findings may be useful in predicting *a priori* which classes of proteins will be most affected by therapeutic inhibitors of eIF4A1 or eIF4E.

DISCUSSION

Significant efforts have been made to identify translational targets of eIF4F during transformation and cancer progression. Still, the rules governing eIF4F-dependent translation initiation and the key drivers of malignant phenotypes are not well understood. We demonstrate that although the eIF4F subunits eIF4A1 and eIF4E commonly promote melanoma proliferation and invasion, they have distinct effects on the melanoma proteome.

Proteomics defines eIF4F targets that contribute to melanoma phenotypes

Mass spectrometry is typically insensitive to small fold-changes, but recently developed MS3 overcomes this limitation (23) and enables reliable detection of physiological protein changes. We leveraged this technology to generate the first eIF4A1- and eIF4E-dependent proteomes. These datasets provide a new layer of insight into the phenotypic effects of eIF4A1 and eIF4E in cancer cells. A proteomic approach has distinct advantages over translation efficiency-based methods. The first is that for protein-coding genes, the proteins themselves, not mRNAs, are the primary effectors of biological processes and are thus much more closely related to cellular phenotypes. The second is that ribosome occupancy is only one of many factors contributing to cellular protein levels. Thus, changes in ribosome occupancy don’t always correspond with altered protein levels. The major limitation to proteomics is that it can be difficult to discern direct from indirect targets. We overcame this by performing an integrative mRNA analysis that enriched for direct translational targets. Still, integration of RNA expression, ribosome occupancy and proteomic data will be required to generate a complete model of eIF4F-dependent cancer formation and progression.

eIF4E and eIF4A1 have distinct effects on the proteome

Binding of eIF4E to the m^7G cap (32) recruits eIF4G (33). eIF4G subsequently recruits 43S subunits and eIF4A (34), which melts local secondary structure to facilitate 43S scanning (35). These coordinated events are considered the critical steps in cap-dependent translational regulation. Because these three components are tightly associated, it is logical that knockdown of any of these factors could lead to common effects on protein translation.

Though a few eIF4A1- and eIF4E-specific targets have been identified (22), it was surprising that eIF4A1 and eIF4E proteomes were strongly discordant. Depletion of eIF4A1, in particular, had many effects that were not shared by eIF4E. While opposing regulation at the mRNA level may mask some eIF4E-dependent protein expression changes, it is likely that the different biochemical activities of eIF4E and eIF4A within the eIF4F complex or eIF4F-

independent functions explain factor-specific dependencies. For example, eIF4A, not eIF4E, associates with mRNAs during the pioneer round of translation (36), which is required for mRNA quality control via nonsense-mediated decay.

Combinatorial models of eIF4F function on target mRNAs

Our data demonstrate that eIF4A1 and eIF4E target separate transcripts based on distinct sequence and structural features in the 5′UTR, but their shared targets are defined by common features in the CDS and 3′UTR. CDS and 3′UTR features may therefore predict translational responses to eIF4F independently of 5′UTR features. Consistent with our observations, a computational analysis of two published eIF4E overexpression datasets reported several features of the CDS and 3′UTR – including CDS GC content and 3′UTR length - that influence translational responses (17). Thus, CDS and 3′UTR associations may be more robust than 5′UTR features that tend to contribute inconsistently across studies.

The mechanism through which eIF4F is linked to non-5′UTR features has been elusive. Our data support a role for eIF4E and eIF4A in translation inhibition by promoting miNA-mediated repression at the 3′UTR. Given the number of tumor suppressive miRNAs that have been discovered, including miR-211 in melanoma (37), this activity of the eIF4F complex may be critical for cancer progression. However, other predictive features also influenced eIF4F-dependent protein output on a genome-wide scale, and more research is necessary to understand the cooperative or antagonistic interactions among different features on a given transcript.

For example, the rare codon effect is the first evidence that potentially links eIF4F sensitivity to the efficiency of translation elongation. Initiation is often thought of as the rate-limiting step in translation, but elongation can be limiting in certain contexts (38) and ribosome profiling has begun to reveal novel mechanisms through which elongation regulates the proteome (39). This raises the possibility that eIF4F sensitivity depends, in part, on which step of translation (initiation or elongation) is limiting for a given transcript. An alternative explanation for the rare codon effect could be the role of codon usage in mRNA and protein stability, which is still poorly understood (40). Regardless, our data demonstrate that eIF4F sensitivity is a function of translational dynamics across the length of the transcript, not just in the 5′UTR. Thus, we propose that more accurate models of eIF4F dependence will integrate features of the 5′UTR, CDS and 3′UTR that together modulate protein output.

eIF4F inhibition is a promising approach to cancer therapy

eIF4F is frequently and homogeneously overexpressed in many cancers, and in virtually all cells of a tumor mass (41). Thus, eIF4F inhibition will target greater numbers of tumor cells than therapies that target subclonal genetic or gene expression changes. Moreover, cancer cells can become addicted to elevated levels of protein synthesis (42), potentially creating a therapeutic window to selectively target them.

Molecules that inhibit the eIF4E-cap interaction (43), eIF4E-eIF4G interaction (44) and eIF4A helicase activity (45,46) are effective in preclinical models. An antisense oligonucleotide inhibitor of eIF4E has shown particular promise (47,48) and is currently in Phase II clinical trials as part of combination therapies for prostate (NCT01234025) and

non-small cell lung (NCT01234038) cancers. Our data suggest that therapeutically targeting different eIF4F subunits in the same cancer will lead to disparate molecular outcomes that influence on- and off-target effects. Additionally, we observed a robust increase in expression of proteins required for oxidative phosphorylation in eIF4A1- and eIF4E-depleted melanoma, whereas the opposite was found in eIF4E-depleted MCF7 human breast cancer cells (22,49). The data from both cell types are compelling, and the discrepancy likely reflects differences in baseline molecular or metabolic state of the different cell types. Thus, the effects of eIF4F inhibitors should not only be evaluated within cancer-subtypes, but among cancer subtypes with distinct molecular makeups. Ultimately, it is possible that rational selection of eIF4F inhibitors could lead to greater therapeutic effects and fewer off-target effects than general inhibition of the upstream signaling pathways that converge on eIF4F.

Supplementary Material

Refer to Web version on PubMed Central for supplementary material.

Acknowledgments

FUNDING STATEMENT: This work was supported by National Institutes of Health grant R01 CA140986 to C.D. Novina. C.E. Joyce was supported by National Institutes of Health training grant T32 CA070083 and postdoctoral fellowship F32 HL124941. A.G. Yanez was supported by National Institutes of Health training grant GM07266 and predoctoral fellowship F31 GM087947.

The authors acknowledge the Flow Cytometry and Confocal and Light Microscopy core facilities (Dana-Farber Cancer Institute), the Thermo Fisher Scientific Center for Multiplexed Proteomics (Harvard Medical School) and the Genomics Platform (Broad Institute) for providing technical assistance and equipment. We thank Drs. Eli Roberson and Guocheng Yuan for critical comments on the manuscript.

References

1. Gingras AC, Raught B, Sonenberg N. eIF4 initiation factors: effectors of mRNA recruitment to ribosomes and regulators of translation. Annu Rev Biochem. 1999 Jan.68:913–63. [PubMed: 10872469]
2. Li BD, McDonald JC, Nassar R, De Benedetti A. Clinical outcome in stage I to III breast carcinoma and eIF4E overexpression. Ann Surg. 1998 May; 227(5):756–61. [PubMed: 9605667]
3. Yoshizawa A, Fukuoka J, Shimizu S, Shilo K, Franks TJ, Hewitt SM, et al. Overexpression of phospho-eIF4E is associated with survival through AKT pathway in non-small cell lung cancer. Clin Cancer Res. 2010 Jan 1; 16(1):240–8. [PubMed: 20008839]
4. Liang S, Zhou Y, Chen Y, Ke G, Wen H, Wu X. Decreased expression of EIF4A1 after preoperative brachytherapy predicts better tumor-specific survival in cervical cancer. Int J Gynecol Cancer. 2014 Jun; 24(5):908–15. [PubMed: 24844222]
5. Tu L, Liu Z, He X, He Y, Yang H, Jiang Q, et al. Over-expression of eukaryotic translation initiation factor 4 gamma 1 correlates with tumor progression and poor prognosis in nasopharyngeal carcinoma. Mol Cancer. 2010 Jan.9:78. [PubMed: 20398343]
6. Petroulakis E, Parsyan A, Dowling RJO, LeBacquer O, Martineau Y, Bidinosti M, et al. p53-dependent translational control of senescence and transformation via 4E-BPs. Cancer Cell. 2009 Nov 6; 16(5):439–46. [PubMed: 19878875]
7. Robichaud N, del Rincon SV, Huor B, Alain T, Petruccelli LA, Hearnden J, et al. Phosphorylation of eIF4E promotes EMT and metastasis via translational control of SNAIL and MMP-3. Oncogene. 2015 Apr 16; 34(16):2032–42. [PubMed: 24909168]
8. Rinker-Schaeffer CW, Graff JR, De Benedetti A, Zimmer SG, Rhoads RE. Decreasing the level of translation initiation factor 4E with antisense RNA causes reversal of ras-mediated transformation

and tumorigenesis of cloned rat embryo fibroblasts. Int J cancer. 1993 Nov 11; 55(5):841–7. [PubMed: 8244582]

9. Boussemart L, Malka-Mahieu H, Girault I, Allard D, Hemmingsson O, Tomasic G, et al. eIF4F is a nexus of resistance to anti-BRAF and anti-MEK cancer therapies. Nature. 2014 Sep 4; 513(7516): 105–9. [PubMed: 25079330]
10. Wagle N, Emery C, Berger MF, Davis MJ, Sawyer A, Pochanard P, et al. Dissecting therapeutic resistance to RAF inhibition in melanoma by tumor genomic profiling. J Clin Oncol. 2011 Aug 1; 29(22):3085–96. [PubMed: 21383288]
11. Hiremath LS, Webb NR, Rhoads RE. Immunological detection of the messenger RNA cap-binding protein. J Biol Chem. 1985 Jul 5; 260(13):7843–9. [PubMed: 3891747]
12. Lin C-J, Malina A, Pelletier J. c-Myc and eIF4F constitute a feedforward loop that regulates cell growth: implications for anticancer therapy. Cancer Res. 2009 Oct 1; 69(19):7491–4. [PubMed: 19773439]
13. Kevil CG, De Benedetti A, Payne DK, Coe LL, Laroux FS, Alexander JS. Translational regulation of vascular permeability factor by eukaryotic initiation factor 4E: implications for tumor angiogenesis. Int J cancer. 1996 Mar 15; 65(6):785–90. [PubMed: 8631593]
14. Hsieh AC, Liu Y, Edlind MP, Ingolia NT, Janes MR, Sher A, et al. The translational landscape of mTOR signalling steers cancer initiation and metastasis. Nature. 2012 May 3; 485(7396):55–61. [PubMed: 22367541]
15. Thoreen CC, Chantranupong L, Keys HR, Wang T, Gray NS, Sabatini DM. A unifying model for mTORC1-mediated regulation of mRNA translation. Nature. 2012 May 3; 485(7396):109–13. [PubMed: 22552098]
16. Truitt ML, Conn CS, Shi Z, Pang X, Tokuyasu T, Coady AM, et al. Differential Requirements for eIF4E Dose in Normal Development and Cancer. Cell. 2015 Jul 2; 162(1):59–71. [PubMed: 26095252]
17. Santhanam AN, Bindewald E, Rajasekhar VK, Larsson O, Sonenberg N, Colburn NH, et al. Role of 3′UTRs in the translation of mRNAs regulated by oncogenic eIF4E--a computational inference. PLoS One. 2009 Jan.4(3):e4868. [PubMed: 19290046]
18. Mamane Y, Petroulakis E, Martineau Y, Sato T-A, Larsson O, Rajasekhar VK, et al. Epigenetic activation of a subset of mRNAs by eIF4E explains its effects on cell proliferation. PLoS One. 2007 Jan.2(2):e242. [PubMed: 17311107]
19. Rubio CA, Weisburd B, Holderfield M, Arias C, Fang E, DeRisi JL, et al. Transcriptome-wide characterization of the eIF4A signature highlights plasticity in translation regulation. Genome Biol. 2014 Jan.15(10):476. [PubMed: 25273840]
20. Larsson O, Li S, Issaenko OA, Avdulov S, Peterson M, Smith K, et al. Eukaryotic translation initiation factor 4E induced progression of primary human mammary epithelial cells along the cancer pathway is associated with targeted translational deregulation of oncogenic drivers and inhibitors. Cancer Res. 2007 Jul 15; 67(14):6814–24. [PubMed: 17638893]
21. Rajasekhar VK, Viale A, Socci ND, Wiedmann M, Hu X, Holland EC. Oncogenic Ras and Akt signaling contribute to glioblastoma formation by differential recruitment of existing mRNAs to polysomes. Mol Cell. 2003 Oct; 12(4):889–901. [PubMed: 14580340]
22. Gandin V, Masvidal L, Hulea L, Gravel S-P, Cargnello M, McLaughlan S, et al. nanoCAGE reveals 5′ UTR features that define specific modes of translation of functionally related MTOR-sensitive mRNAs. Genome Res. 2016 May; 26(5):636–48. [PubMed: 26984228]
23. McAlister GC, Nusinow DP, Jedrychowski MP, Wühr M, Huttlin EL, Erickson BK, et al. MultiNotch MS3 enables accurate, sensitive, and multiplexed detection of differential expression across cancer cell line proteomes. Anal Chem. 2014 Jul 15; 86(14):7150–8. [PubMed: 24927332]
24. Lin WM, Baker AC, Beroukhim R, Winckler W, Feng W, Marmion JM, et al. Modeling genomic diversity and tumor dependency in malignant melanoma. Cancer Res. 2008 Feb 1; 68(3):664–73. [PubMed: 18245465]
25. Khosravi S, Tam KJ, Ardekani GS, Martinka M, McElwee KJ, Ong CJ. eIF4E is an adverse prognostic marker of melanoma patient survival by increasing melanoma cell invasion. J Invest Dermatol. 2015 May; 135(5):1358–67. [PubMed: 25562667]

26. Carter JH, Deddens JA, Spaulding NR IV, Lucas D, Colligan BM, Lewis TG, et al. Phosphorylation of eIF4E serine 209 is associated with tumour progression and reduced survival in malignant melanoma. Br J Cancer. 2016 Feb 16; 114(4):444–53. [PubMed: 26882068]
27. Bettum IJ, Gorad SS, Barkovskaya A, Pettersen S, Moestue SA, Vasiliauskaite K, et al. Metabolic reprogramming supports the invasive phenotype in malignant melanoma. Cancer Lett. 2015 Sep 28; 366(1):71–83. [PubMed: 26095603]
28. Felding-Habermann B. Integrin adhesion receptors in tumor metastasis. Clin Exp Metastasis. 2003 Jan; 20(3):203–13. [PubMed: 12741679]
29. Appert-Collin A, Hubert P, Crémel G, Bennasroune A. Role of ErbB Receptors in Cancer Cell Migration and Invasion. Front Pharmacol. 2015 Jan.6:283. [PubMed: 26635612]
30. Mathonnet G, Fabian MR, Svitkin YV, Parsyan A, Huck L, Murata T, et al. MicroRNA inhibition of translation initiation in vitro by targeting the cap-binding complex eIF4F. Science. 2007 Sep 21; 317(5845):1764–7. [PubMed: 17656684]
31. Fukao A, Mishima Y, Takizawa N, Oka S, Imataka H, Pelletier J, et al. MicroRNAs trigger dissociation of eIF4AI and eIF4AII from target mRNAs in humans. Mol Cell. 2014 Oct 2; 56(1): 79–89. [PubMed: 25280105]
32. Sonenberg N, Morgan MA, Merrick WC, Shatkin AJ. A polypeptide in eukaryotic initiation factors that crosslinks specifically to the 5′-terminal cap in mRNA. Proc Natl Acad Sci U S A. 1978 Oct; 75(10):4843–7. [PubMed: 217002]
33. Mader S, Lee H, Pause A, Sonenberg N. The translation initiation factor eIF-4E binds to a common motif shared by the translation factor eIF-4 gamma and the translational repressors 4E-binding proteins. Mol Cell Biol. 1995 Sep; 15(9):4990–7. [PubMed: 7651417]
34. Imataka H, Sonenberg N. Human eukaryotic translation initiation factor 4G (eIF4G) possesses two separate and independent binding sites for eIF4A. Mol Cell Biol. 1997 Dec; 17(12):6940–7. [PubMed: 9372926]
35. Ray BK, Lawson TG, Kramer JC, Cladaras MH, Grifo JA, Abramson RD, et al. ATP-dependent unwinding of messenger RNA structure by eukaryotic initiation factors. J Biol Chem. 1985 Jun 25; 260(12):7651–8. [PubMed: 3838990]
36. Chiu S-Y, Lejeune F, Ranganathan AC, Maquat LE. The pioneer translation initiation complex is functionally distinct from but structurally overlaps with the steady-state translation initiation complex. Genes Dev. 2004 Apr 1; 18(7):745–54. [PubMed: 15059963]
37. Levy C, Khaled M, Iliopoulos D, Janas MM, Schubert S, Pinner S, et al. Intronic miR-211 assumes the tumor suppressive function of its host gene in melanoma. Mol Cell. 2010 Dec 10; 40(5):841–9. [PubMed: 21109473]
38. Chu D, Kazana E, Bellanger N, Singh T, Tuite MF, von der Haar T. Translation elongation can control translation initiation on eukaryotic mRNAs. EMBO J. 2014 Jan 7; 33(1):21–34. [PubMed: 24357599]
39. Richter JD, Coller J. Pausing on Polyribosomes: Make Way for Elongation in Translational Control. Cell. 2015 Oct 8; 163(2):292–300. [PubMed: 26451481]
40. Zhou M, Guo J, Cha J, Chae M, Chen S, Barral JM, et al. Non-optimal codon usage affects expression, structure and function of clock protein FRQ. Nature. 2013 Mar 7; 495(7439):111–5. [PubMed: 23417067]
41. Ramon Y, Cajal S, De Mattos-Arruda L, Sonenberg N, Cortes J, Peg V. The intra-tumor heterogeneity of cell signaling factors in breast cancer: p4E-BP1 and peIF4E are diffusely expressed and are real potential targets. Clin Transl Oncol. 2014 Nov; 16(11):937–41. [PubMed: 25060567]
42. Hsieh AC, Costa M, Zollo O, Davis C, Feldman ME, Testa JR, et al. Genetic dissection of the oncogenic mTOR pathway reveals druggable addiction to translational control via 4EBP-eIF4E. Cancer Cell. 2010 Mar 16; 17(3):249–61. [PubMed: 20227039]
43. Ghosh B, Benyumov AO, Ghosh P, Jia Y, Avdulov S, Dahlberg PS, et al. Nontoxic chemical interdiction of the epithelial-to-mesenchymal transition by targeting cap-dependent translation. ACS Chem Biol. 2009 May 15; 4(5):367–77. [PubMed: 19351181]

44. Moerke NJ, Aktas H, Chen H, Cantel S, Reibarkh MY, Fahmy A, et al. Small-molecule inhibition of the interaction between the translation initiation factors eIF4E and eIF4G. Cell. 2007 Jan 26; 128(2):257–67. [PubMed: 17254965]

45. Low W-K, Dang Y, Schneider-Poetsch T, Shi Z, Choi NS, Merrick WC, et al. Inhibition of eukaryotic translation initiation by the marine natural product pateamine A. Mol Cell. 2005 Dec 9; 20(5):709–22. [PubMed: 16337595]

46. Tsumuraya T, Ishikawa C, Machijima Y, Nakachi S, Senba M, Tanaka J, et al. Effects of hippuristanol, an inhibitor of eIF4A, on adult T-cell leukemia. Biochem Pharmacol. 2011 Mar 15; 81(6):713–22. [PubMed: 21219881]

47. De Benedetti A, Joshi-Barve S, Rinker-Schaeffer C, Rhoads RE. Expression of antisense RNA against initiation factor eIF-4E mRNA in HeLa cells results in lengthened cell division times, diminished translation rates, and reduced levels of both eIF-4E and the p220 component of eIF-4F. Mol Cell Biol. 1991 Nov; 11(11):5435–45. [PubMed: 1922056]

48. Graff JR, Konicek BW, Vincent TM, Lynch RL, Monteith D, Weir SN, et al. Therapeutic suppression of translation initiation factor eIF4E expression reduces tumor growth without toxicity. J Clin Invest. 2007 Sep; 117(9):2638–48. [PubMed: 17786246]

49. Morita M, Gravel S-P, Chénard V, Sikström K, Zheng L, Alain T, et al. mTORC1 controls mitochondrial activity and biogenesis through 4E-BP-dependent translational regulation. Cell Metab. 2013 Nov 5; 18(5):698–711. [PubMed: 24206664]

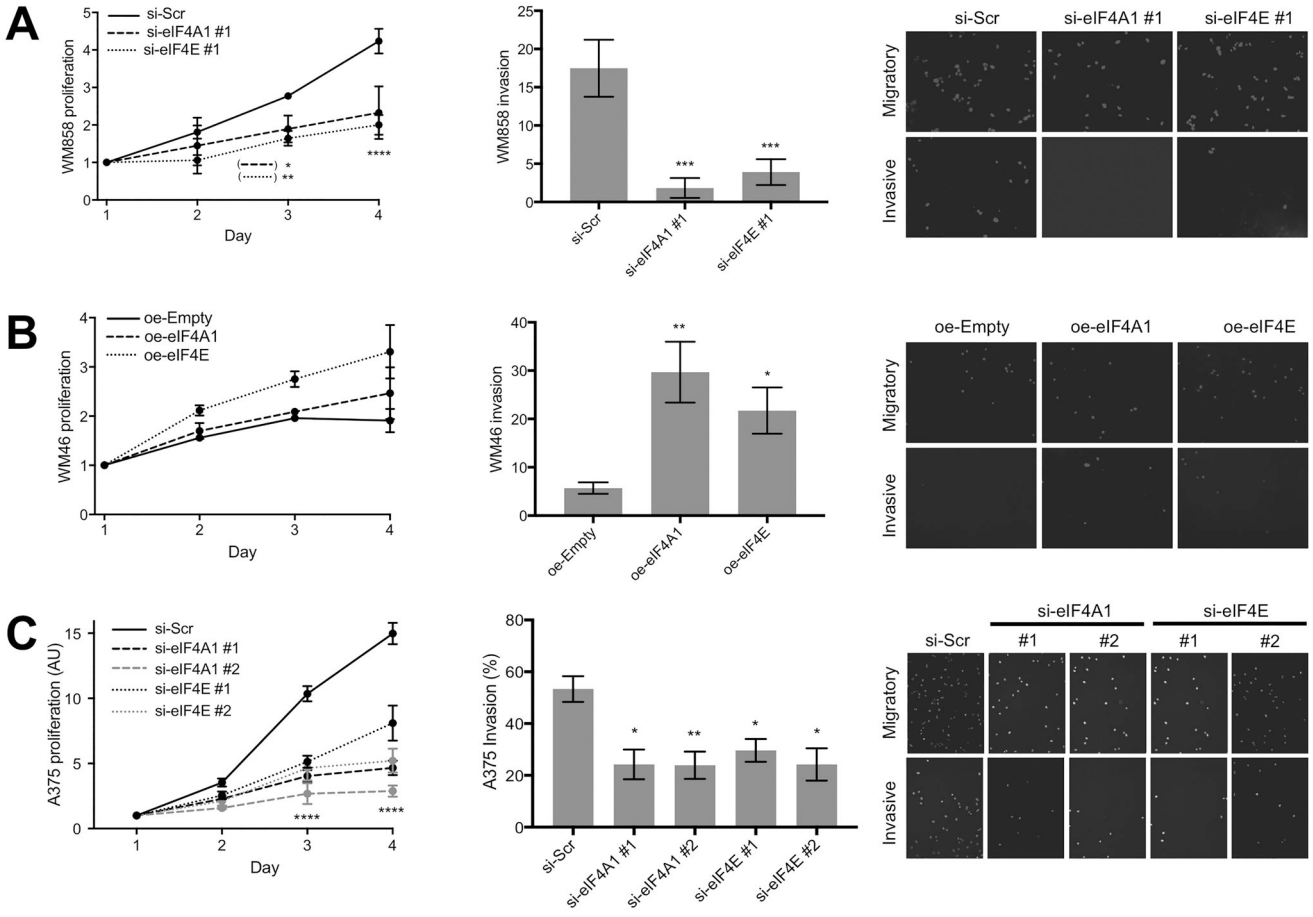

Figure 1. eIF4A1 and eIF4E are positive regulators of melanoma proliferation and invasion

Proliferation rates (left) and invasion rates (center) with representative images (right) for the (A) WM858 MSTC treated with siRNAs against eIF4A1 (si-eIF4A1 #1), eIF4E (si-eIF4E #1) or scrambled sequence (si-Scr), (B) WM46 MSTC treated with mammalian expression vectors encoding eIF4A1 (oe-eIF4A1), eIF4E (oe-eIF4E) or empty vector (oe-Empty) and (C) A375 melanoma cell line treated with si-Scr, or one of two independent siRNAs against eIF4A1 and eIF4E. Proliferation values were normalized to day one, and plotted relative to si-Scr. Percent invasion is calculated as the number of invasive cells on a matrigel-coated filter relative to the number of migratory cells on an uncoated control filter seeded at the same density. Error bars = standard error of the mean (SEM), n≥3 replicates/treatment, *p<0.05, **p<0.01, ***p<0.001, ****p<0.0001.

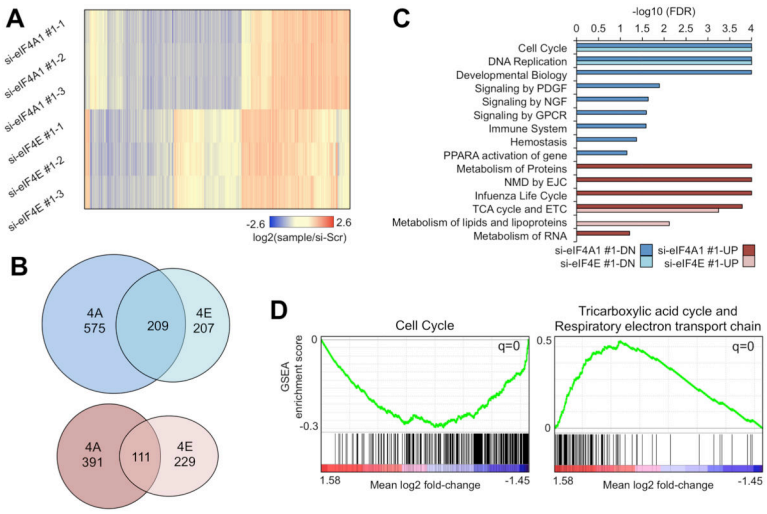

Figure 2. eIF4A1 and eIF4E commonly regulate cell cycle and oxidative phosphorylation

(A) Heatmap, hierarchically clustered by sample and gene, showing log2 fold-change relative to si-Scr for differentially expressed proteins in A375 treated with si-eIF4A1 #1 or si-eIF4E #1 (log2 fold-change ≥|1.25|, FDR<0.1). (B) Overlap between decreased (blue) or increased (red) proteins with each siRNA treatment. (C) Enriched Reactome pathways among decreased or increased proteins in the si-eIF4A1 #1 or si-eIF4E #1 treatments. In cases where multiple enriched pathways were under the same parent pathway, only the parent pathway has been shown. For complete enrichment results, see Table S1. (D) Enrichment plots for the commonly regulated Reactome categories, Cell Cycle and Tricarboxylic Acid Cycle/Eelectron Transport Chain (TCA/ETC). Black lines indicate the rank positions of category members based on average fold-change in all knockdown treatments. NMD=nonsense mediated decay, EJC=exon junction complex.

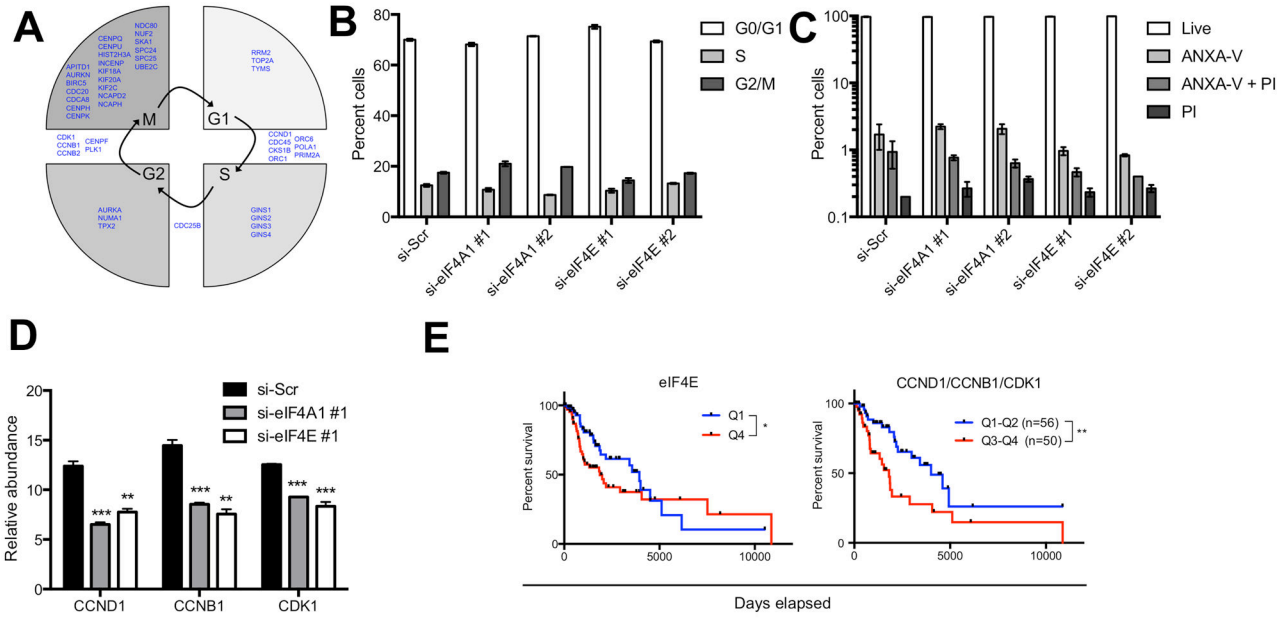

Figure 3. The eIF4F-dependent cell cycle network influences melanoma patient survival

(A) Commonly regulated proteins that are annotated to the Reactome Cell Cycle pathway mapped onto phases of the cell cycle based on their Reactome subcategory annotations. Proteins that mediate transitions or function in multiple phases are shown in the gaps. Blue font denotes decreased protein expression level. (B) The frequency of each cell cycle phase in A375 cells treated with si-Scr, si-eIF4A1 or si-eIF4E (error bars = SEM, n=3 replicates). (C) The frequency of cells expressing the apoptotic marker, annexin 5 (ANXA5), or dead cell marker, propidium iodide (PI), in A375 cells treated with si-Scr, si-eIF4A1 or si-eIF4E (error bars = SEM, n=3 replicates). (D) Kaplan-Meier survival curves generated from 328 cutaneous melanoma patients in TCGA. Patients used to generate the eIF4E curve were in the first or fourth quartiles based on normalized expression of the indicated protein (n=82 per group). Patients used to generate the CDK1/CCNB1/CCND1 curve had above-median and below-median expression of all three proteins. The less stringent cutoff was applied to obtain a roughly equivalent sample size. For (B–D), *p<0.05, **p<0.01, ***p<0.001, ****p<0.0001.

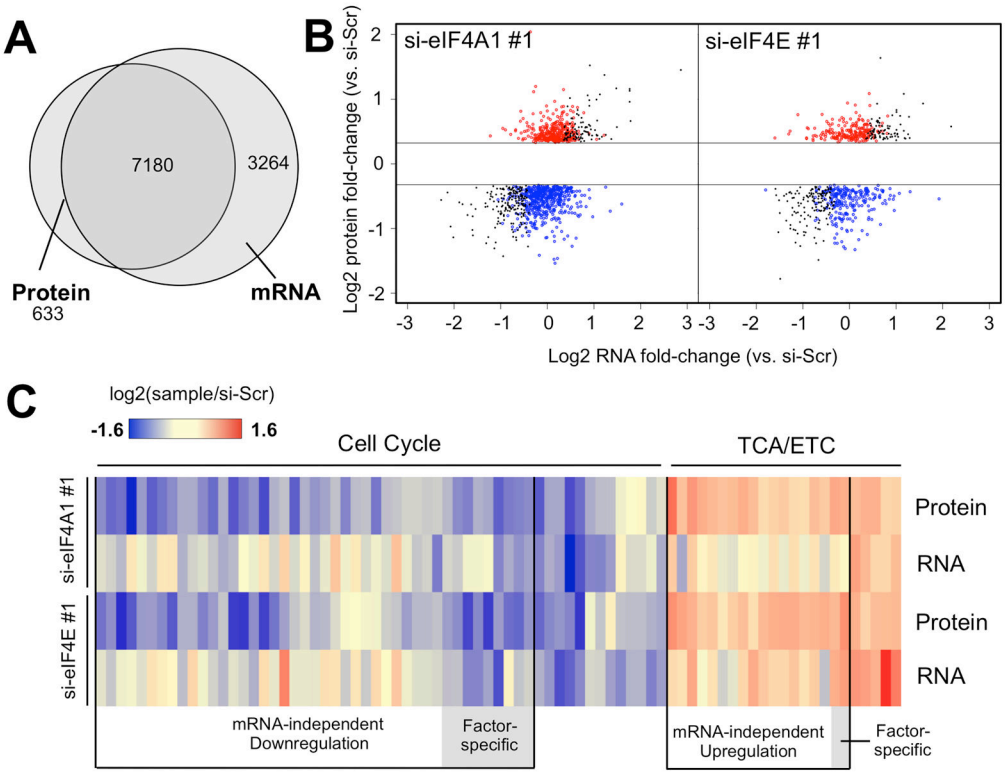

Figure 4. Integrated RNA and protein analysis defines direct translational targets of eIF4A1 and eIF4E

(A) Overlap in transcripts detected in A375 by RNA-seq (FPKM≥1, n=2 biological replicates per treatment) and MS3 (peptides≥1, n=3 biological replicates per treatment). (B) Average log2 protein versus average log2 mRNA fold-change for differentially expressed proteins in si-eIF4A1 #1 or si-eIF4E #1 treatments. Red and blue points denote proteins that do not have a concordant change in mRNA level (mRNA fold-change in 2 biological replicates ≤1.25 and/or FDR<0.1 for increased proteins, ≥ −1.25 and/or FDR<0.1 for decreased proteins). (C) Manually-clustered heatmap showing log2 fold-change at the mRNA and protein level for differentially expressed proteins that are annotated to the commonly enriched Cell Cycle or TCA/ETC Reactome pathways. ‘Factor-specific’ refers to proteins that are directly regulated by one factor and indirectly regulated by the other.

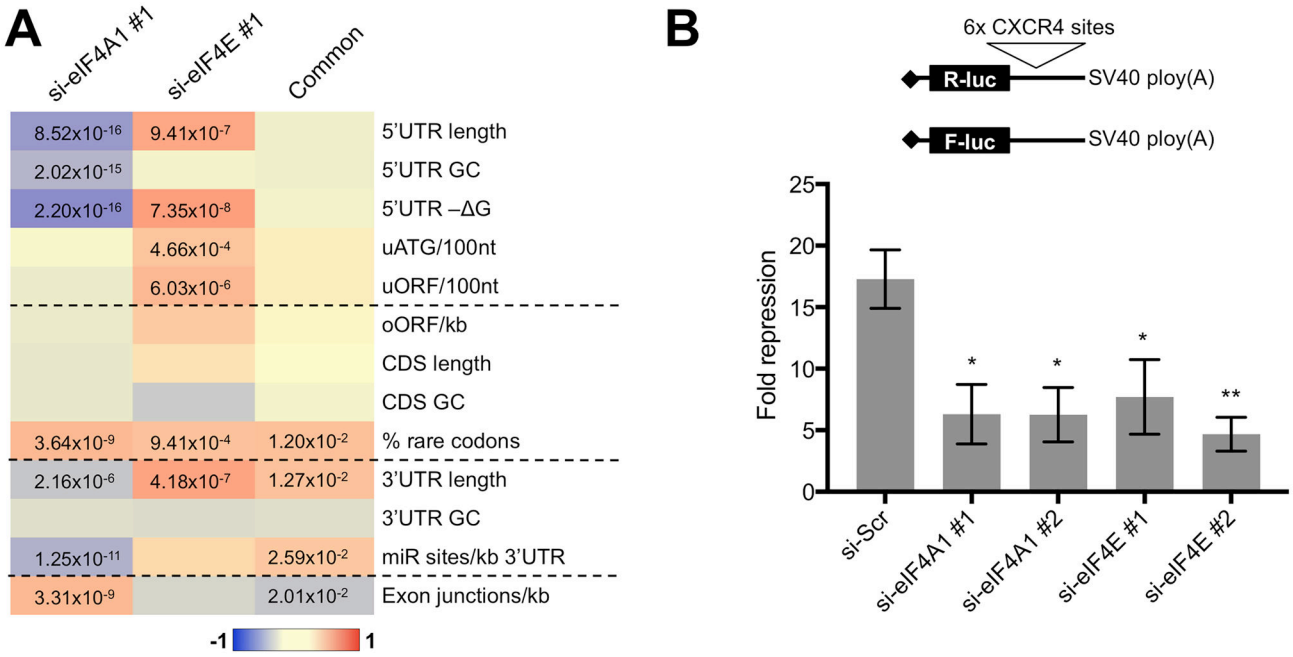

Figure 5. CDS and 3′UTR features predict direct regulation by eIF4A1- and eIF4E

(A) Manually-clustered heatmap of effect sizes (Cliff's D) for thirteen mRNA features among direct targets of eIF4A1, eIF4E, or both factors. Dotted lines demarcate 5′UTR, CDS, 3′UTR and whole transcript features. p-values are shown for features where $p<0.05$ and effect size is greater than 20%. (B) Fold-repression of a miRNA-targeted *Renilla* luciferase reporter relative to a non-targeted firefly luciferase reporter. *$p<0.05$, **$p<0.01$.